

Gerald M. Colver (Primary Contact)
Department of Mechanical Engineering
Iowa State University
2036 Black Engineering Bldg.
Ames, IA 50011
E-mail: gmc@iastate.edu
Tel: 515-294-7572
Fax: 515-294-3261

Robert C. Brown
Departments of Mechanical Engineering
and Chemical Engineering
Iowa State University
286 Metals Development Bldg.
Ames, IA 50011
E-mail: rcbrown@iastate.edu
Tel: 515-294-7934
Fax: 515-294-3091

Huawei Shi
Department of Mechanical Engineering
Iowa State University
2025 Black Engineering Bldg.
Black Engineering Bldg.
Ames, IA 50011
E-mail: shihw@iastate.edu
Tel: 515-294-1423
Fax: 515-294-3261

Darren Saw-Choon Soo
Department of Mechanical Engineering
Iowa State University
2025 Black Engineering Bldg.
Black Engineering Bldg.
Ames, IA 50011
E-mail: ssoo@iastate.edu
Tel: 515-294-1423
Fax: 515-294-3261

Improving Efficiency of a Counter-Current Flow Moving Bed Granular Filter

Keywords: particulate filtration, granular filter, moving bed, hot gas clean-up, dust capture

Introduction

The U.S. Department of Energy is developing advanced coal-fired power cycles. One important process is the removal of fine particles from high-temperature and high-pressure gas streams to satisfy gas turbine fuel quality requirements. Ceramic candle barrier filters and granular bed filters are the most promising approaches to hot gas clean-up for advanced coal conversion technologies (Mustonen et al., 1991; Wilson & Hass, 1994). Granular bed filters are more attractive because they employ low-cost refractory particles as filter media and offer the prospect for constant pressure drop if the filter is operated as a moving bed. In general, there are two types of granular bed filters: fixed bed and moving bed. Moving bed granular filters can renew the filtration media continuously. This advantage makes unnecessary periodical shutdown of the filter to renew the filter media.

Previous research offers considerable anecdotal evidence that dust cake formation is extremely important in achieving high collection efficiency for granular bed filters (Squires and Pfeffer, 1970). However, experimental and theoretical studies of this interfacial phenomenon are almost totally absent in the published literature. Further hampering the usefulness of existing experimental data to the design of commercial moving bed granular filters are the conditions under which most of the data were obtained. Usually no attempt was made to simulate the hydrodynamic conditions of hot gas clean-up. Thus, this data correlated in terms of such dimensionless parameters as Stokes number, Peclet number, and Grashof number, gives results outside the operating range of

commercial filters. This research is an attempt to investigate performance of a moving bed granular filter developed at Iowa State University.

Objective

The goal of this research is to improve the performance of moving bed granular filters for gas cleaning at high temperatures and pressures. A second goal of the research is to optimize the performances of both solids and gas filtering processes through appropriate use of granular bed materials, particle sizes, feed rates etc. in a factorial study. These goals are directed toward applications of advanced coal-fired power cycles under development by the U.S. Department of Energy including pressurized fluidized bed combustion and integrated gasification/combined cycles based on gas turbines and fuel cells. Only results for particulate gas cleaning are reported here.

Specific objectives of this research include:

- Understand the interfacial phenomena of dust cake formation in moving bed filters
- Develop performance correlations applicable to high temperatures and pressures
- Develop granular filters that exploit dust cakes to improve collection efficiency

Approach

A cold flow, axially symmetric bed has been designed to simulate performance of filters operated at high temperatures (1088 K) and elevated pressures (10 atmospheres) by the use of similarity rules satisfying four dimensionless parameters for filter hydrodynamics. The filter utilizes counter-current flow of gas and media in the bed. This technique establishes quasi-steady dust capture at the interface and within the bed. Granular bed filters are attractive because they employ simple particles (often low-cost refractory materials) as filter media and offer the prospect for constant pressure drop. The filter is continuously renewed on the upstream side of the bed and swept away on the downstream side. The advantage of quasi-steady dust capture is the avoidance of periodic variation in efficiency and pressure drop inherent in most barrier filters.

Theory of Filtration: The theory of granular bed filtration is essentially that of barrier filters. In principle, several separation mechanisms can contribute:

- Inertial impaction – a dust particle is too large to follow a curved streamline around a granule and its inertia carries it into the granule.
- Diffusion – Brownian motion of a dust particle superimposed on the bulk flow of the gas bring the particle into collision with a granule.
- Gravity – dust particles settle from the gas flow under the action of gravity.
- Interception – a dust particle following a streamline close to a granule slides into the granule.
- Electrostatic attraction – dust particles carrying a different electrostatic charge than bed granules will be attracted to the granules.

Performance of particulate filters are often expressed in terms of the particle collection efficiency, η

$$\eta = 1 - \frac{\text{mass of dust exiting}}{\text{mass of dust entering}} \quad (1)$$

Collection efficiency of a moving granule bed filter is a function of the granule size, superficial velocity at the filter face area, velocity of the granules, and the properties of the gas and dust (Saxena et al., 1985). For a clean filter, collection efficiency is also a function of bed depth. The presence of dust cake should not only increase collection efficiency but may shift collection to an essentially surface phenomenon. However, virtually no experimental information is available on the effect of dust cake on filtration mechanisms.

In the present study, particle collection efficiency could be determined by three methods: (1) isokinetic particle sampling upstream and downstream from the bed at the centerline; (2) weight loss from the flyash feeder (before and after a run); and (3) laser attenuation measurement of particle concentration just upstream and downstream from the bed filter. In this study, centerline isokinetic particle sampling (1) was the primary method used with weight loss (2) applied as a check. The laser attenuation experienced problems of long-term drift as well as uncertainties inherent in the method.

For high performance filters, efficiency is more conveniently expressed as the penetration, P :

$$P = 1 - \eta \quad (2)$$

which simply indicates the fraction of dust completely penetrating the filter

Similitude analysis: Similitude analysis is based on dimensionless parameters to describe filter performance (Freidlander, 1977). Although there are several kinds of collection mechanism as noted above, most moving bed granular filters, including the filter studied in this research, operate in a regime where inertial impaction is the main collection mechanism. For inertial impaction filters, collection efficiency can be expressed with three dimensionless parameters as (Freidlander, 1977).

$$\eta = f(St, Re, R) \quad (3)$$

In the case of a granular filter, two additional dimensionless parameters are required to describe the hydrodynamics of the moving bed giving five dimensionless parameters to control (Glicksman, 1993):

$$\text{St: Stokes number, } St = \frac{\rho_p \cdot d_p^2 \cdot U \cdot C_s}{9 \cdot \mu \cdot d_g} \quad (4)$$

$$\text{Re: Reynolds number based on granule diameter, } Re = \frac{\rho_f \cdot U \cdot d_g}{\mu} \quad (5)$$

$$\text{R: Interception number, } R = \frac{d_p}{d_g} \quad (6)$$

$$R_{rho}: \text{The ratio granule density to fluid density, } R_{rho} = \frac{\rho_g}{\rho_f} \quad (7)$$

$$\text{Froude number, } Fr = \frac{U^2}{g \cdot d_g} \quad (8)$$

where ρ_p =particle (fly ash) density, ρ_f =fluid (air) density, d_p =particle (fly ash) average diameter, d_g = bed granule diameter, U = Superficial velocity, $Cs=1$, Cunningham factor and μ :=fluid (air) viscosity. Let subscripts 1 and 2 distinguish the physical properties of two filters, model and prototype and set the dimensionless ratios equal for similitude. Algebraic manipulation of the above dimensionless variables yields property relationships convenient for establishing hydrodynamic similarity between the filters:

$$\frac{\rho_{p1}}{\rho_{p2}} = \frac{\rho_{g1}}{\rho_{g2}} = \frac{\rho_{f1}}{\rho_{f2}} \quad \frac{U_1}{U_2} = \left(\frac{v_1}{v_2} \right)^{\frac{1}{3}} \quad \frac{d_{p1}}{d_{p2}} = \frac{d_{g1}}{d_{g2}} = \left(\frac{v_1}{v_2} \right)^{\frac{2}{3}} \quad (9)$$

where $v = \mu/\rho_f$ (kinematic viscosity of the fluid). Table 1 gives an example-calculated result for model and prototype to achieve similitude. In the present study the prototype predictions were verified only at near atmospheric pressure and room temperature. However, our results should be useful for estimating design of filters and for suggesting operating conditions of the prototype.

Project Description

High pressure simulation tests were carried out using the cold-flow model (STP) of a moving bed granular filter. Filter collection efficiency pressures in the cold flow model were extended to 262 kPa (38 psia). Inlet ash concentration, outlet ash concentration, filter collection efficiency and pressure drop across the bed were important experimental data collected. Seven experiments were conducted to investigate the effects of several factors on filter collection efficiency. These factors include

1. Ash feed rate to granule flow rate (“mass dust ratio”)
2. Size of granules used a filter media
3. Bed pressure
4. Superficial velocity at the filter interface

The results of cold model tests provide information important to future prototype tests performed at high pressure and high temperature conditions. The simulation results also can provide important information for the design of moving bed filters for commercial applications.

Our moving granular bed filter utilizes a counter-current flow design to capture fly ash (nominal 12 μm diameter) at the interface and within the bed of a conically shaped granular bed of 2-5 mm silica particles (Figs. 1-a,b). The facility is fully instrumented using computer data acquisition. Fresh granular material is fed in at the top of the bed with dirty granular material removed from the bottom of the bed. Fly ash laden air enters the bed through a 0.114 m (4.5 in) diameter inlet feed pipe 2.134 m (84 in) in length while cleaned air exits from the top of the bed (counter-flow to the granular material flow) through a pipe of similar length and diameter (Fig. 2). The 0.302 m (11.9-in)

id aluminum bed housing together with the system piping components are designed to handle pressures up to 206.8-241 kPa gage (30-35 psig), suitable for similitude (cold flow) studies. An auger feed controls the flow rate of fly ash from a vibrated reservoir located upstream and just at the entrance to the inlet feed pipe. A unique design feature of our filter is the buildup of dust near the gas-bed interface of the filter to improve particle capture efficiency while the natural conical shape of the bed itself helps to compensate for the increase in pressure drop resulting from the captured particles. Airflow strengtheners (fins) located inside the housing (Fig. 1-a) direct the inlet airflow at the interface thereby reducing disturbances of captured dust while an inner cone placed in the bed itself improves the control of granular flow.

The flow rate characteristics of the filter with system pressure with/without a granular bed of 4-5 mm pebbles is shown in Fig. 3. For a fixed source pressure of 353 kPa (51.2 psia), the system flow rate was limited to a maximum air flow rate of 41 SCFM up to a pressure of about 138 kPa (20 psia) and then steadily declines with increasing system pressure. This limited the useful range of testing of higher system pressures to about 262 kPa (38 psia) because of the requirement of the critical minimum air (saltation) velocity needed to entrain the fly ash.

The fly ash used in experiments had an average diameter of 11.46 μm and density of 2400 kg/m^3 . Two sizes of spherical bed granules 2 and 4 mm diameter were used in the experiments. Both had a density of 2450 kg/m^3 .

Results

Results from this research are broken down into two studies: (1) the experimental development of the facility, and (2) performance of particle collection efficiency and pressure drop of the moving bed granular filter at near atmospheric pressure and slightly elevated pressures to 23.16 psig (159.7 kPa gage).

The initial development of the facility study (1) is reviewed in the following paragraphs. A total of three years was required in which construction of the moving bed filter was completed, instrumentation installed and tested, shake down runs performed, improvements made to the granular flow regulating system, and efforts made to increase accuracy of the laser-based and particle sampling measurements. Various barriers associated with operating the facility at elevated pressures were overcome including problems of leakage at optical ports and joints, solids control, and solids/gas measurement using data acquisition. Figure 4-top illustrates the problem of deposition of ash at the feeder located upstream of the bed (cf. Fig. 2-item 16). This was an ongoing problem associated with dispersion of the fly ash and maintaining flyash entrainment, i.e. running the system above salutation conditions. To aid dispersion of flyash, the inlet air was a jet directed at the auger discharge exit. Deposition on the walls of the duct upstream from the bed was an issue involving validating the flow rate of fly ash (Fig. 4-bottom). To minimize sample loss error, the inlet sampling probe was positioned near the bed. It was possible to correct for wall deposition losses in calculating bed collection efficiency by collecting deposited flyash using a special “chimney-sweep” broom following a run.

An uncertainty analysis of the fly ash particle concentration showed that laser-based results (laser system not shown in Fig. 2) could be as large as 50-100%. For this reason, and because of erratic and unexplained long-term light drift in signal, the laser attenuation technique was subsequently

used only to monitor dust flow. During evaluation of the laser beam system, special precautions were taken to keep the windows and passageways of the laser beam clean with small jets of air and painting the pathway walls with low reflecting black paint. Thermal drift was found not to be an issue by testing the beam intensity over extended periods of time. The drift problem of signal remained unresolved.

Several practical design problems were also solved during latter stages of development of the system such as feed control of fly ash and granular material in an elevated pressure system (e.g. using airless L-valve). The air lock issue for feeding fly ash by auger into the pressurized duct was solved by placing the entire feed assembly in a sealed chamber at the pressure of the system. During the three-year period, the facility has undergone select stages of testing and perfecting of the apparatus. A double cone shaped granular flow diverter (Fig.2, item 20) was installed later during trial experiments to aid bed interface flow and to reduce the total quantity of granular material needed over several hours of continuous operations. Early tests with a Plexiglas bed showed that the fins placed around the shell of the bed (Fig 1-a) would straighten the airflow perpendicular to the bed surface reducing entrainment of fly ash by swirling air.

A more recent issue involved the non-optimal behavior of the granular bed itself. Under some conditions of air, granular and fly ash flow rates, steady-state operation of the bed could not be achieved. Following startup of the bed, a rapid decrease in pressure drop across the bed occurred followed by a steady increase in pressure drop in which steady state particle collection could not be achieved over periods of hours. It is speculated that this behavior might be caused by a dead zone of non flowing granular material in the downcomer of the bed below the screen exit (Fig. 1-a) under certain operating conditions of air flow rate, granular particle density and size, and (present) downcomer and feed tube diameters. The observations that filter efficiency degraded with decreasing particle size and increasing gas velocity suggested that degraded performance was related to fluidization of granules somewhere in the filter. Calculation of the ratio of superficial velocity to minimum fluidization velocity (U/U_{mf}) in the granule downcomer revealed degraded performance when particles in the downcomer would be expected to fluidize ($U/U_{mf} > 1$). Although the reasons for this are not fully understood, it seems reasonable that the expanding bed allows more dust to escape through voids, causing decreased filtration efficiency. This escaping dust is likely to lodge in the dead zones of the moving bed, causing increasing pressure drop.

Above-atmospheric pressure study: Results for the second study (2) are divided into above-atmospheric bed operating pressure to 262 kPa (38 psia) and near-atmospheric bed operating pressure using statistical factorial design having up to four test variables: granular flow rate, interfacial velocity, inlet concentration of fly ash dust, and granular size (Vardeman,1994). Details of the above-atmospheric bed pressure study are given in the thesis of Shi (2002). The results for isokinetic sampling both for near-atmospheric and above-atmospheric pressures give filtration efficiencies as high as 99.9% ($\pm 0.1\%$) and typical bed pressure drop across the bed of 6.9 kPa (1.0 psi). Interfacial gas velocity not exceeding 0.4 m/s played a key role in reaching steady state operating conditions.

Figures 5-a shows direct evidence of fly ash dust cake buildup at the bed surface interface using 4 mm spherical glass beads. This particular run had a mass dust ratio (dust feed rate/granular bed feed rate) of 9.8%. The photographs were made with a borescope. Figure 5-b shows that beads below

the interface remain clean. Cake buildup was not observed for smaller dust ratios in which case bed particles might show flaking, a heavily coating, or a light coating of fly ash depending on the various running conditions.

Similarity laws Eqs. (9) were tested at modest pressures and room temperature using the data in Table 2 in which all four experiments satisfy (nearly) similitude conditions. The bed contained 4 mm spherical glass particles. Average bed pressures from the pressure transducer showed fluctuations of less than 2.5% in all runs. The combination of different levels of ash flow rate and granule flow rate gives four values of mass dust ratio, 11.04%, 6.89%, 5.08% and 3.33%. Figure 6 shows the bed efficiency for these tests with time. A factorial statistical analysis supports the conclusion that when operating at these mass dust ratios satisfying similitude, the filter is not strongly influenced by either dust-to-granular ratio or time. The bed reached and maintained steady state conditions.

Pressure drop across the bed is important for assessing pumping requirements of the system and for tracking buildup of dust in the bed over time. For a moving bed, a steady or quasi-steady state is expected to be reached when the amount of fly ash entering the filter equals the amount of ash exiting the bed along with the granules from the bottom of the filter. The pressure drop measured against time is a criterion for steady state. For the four tests in Table 2, Fig. 7 indicates that pressure drop reaches steady state in 5-20 minutes after starting the experiment. For the remaining time, the pressure drop increases at a small but constant rate. A possible explanation for the increase is that the ash captured on granules in the bed reaches a quasi-steady state pressure drop in a relatively short amount of time. It is noted that steady state is achieved for all dust mass ratios. Figures 8 and 9 indicate that operation with small 2mm beads produced a decreasing efficiency and a larger pressure drop that increased monotonically with time following an initial drop during startup. As noted previously, this non-optimum performance associated with smaller particles may be due to a dead zone and/or fluidization in the downcomer of the bed itself.

Separate tests (not shown) carried out at 134 kPa (19.4 psia) and 200 kPa (29 psia) in which steady state was achieved showed that filtration efficiency improves with increasing pressure, and that pressure drop measured as $\Delta p/p$ may reflect dust retention from increasing filtration efficiency. In another test carried out at superficial velocities of 0.20 and 0.42 m/s (measured with respect to bed interface surface) it was found that filtration efficiency degrades with time at the higher superficial velocity while pressure drop across the same bed continuously increased with time following an initial decrease in pressure drop (non-optimal performance).

Near-atmospheric pressure (optimization) study: Central composite design (Vardeman, 1994) was used to configure 16 test runs of the bed at near atmospheric conditions ~ 117 kPa (17 psia) using 4 mm glass beads in the bed. The independent variables were bed granular flow rate, fly ash feed rate, and superficial velocity. The tabulated results for particle collection efficiency and bed pressure drop are given in Table 3. JMP software was used to conduct a standard least square regression analysis of the table data. A full-quadratic model was first regressed followed by a forward stepping regression analysis to improve results.

The resulting equations (not given) for the particle collection efficiency and bed pressure drop covering the data in Table 3 have been plotted respectively in the contour plots of Fig. 10-a at a

superficial velocity of 0.16 m/s and in Fig. 10-b. The dark contour shading indicates bed operating conditions at low particle collection efficiency (~96%) and low bed pressure drop [~ 0.79 kPa (0.1 psid)] while the light shading corresponds to conditions of high bed pressure drop [~ 3.4 kPa (0.5 psid)] and high particle collection efficiency (~100%). Details of the statistical analysis are given in the thesis of Soo (2002). The best performance of the bed (high particle collection efficiency, low bed pressure drop) occurs in regions of lower left to upper right of the contour map. One can estimate a straight line “best performance operating curve” of the bed (high efficiency ~100%; low bed pressure drop ~ 0.79 kPa (0.1 psid) at different combinations of bed granular flow rate (GF) and fly ash feed rate (AF) as

$$GF(kg/hr) = 12.5 AF(kg/hr) + 7.25 \quad \text{“best” performance operating curve,} \quad (10)$$

which applies for near-atmospheric pressure, 4 mm glass beads, and a superficial velocity = 0.16 m/s.

Application

The operational findings for this experimental counter-current moving bed granular filter facility include:

- Filtration efficiency in moving bed granular filter was as high as 99.9% ($\pm 0.1\%$)
- “Best” bed performance operating correlations can be found
- Similitude confirmed for above-atmospheric pressure study
- Visual evidence for importance of dust cake was observed
- Non-optimum performance was indicated by monotonically increasing pressure drop
 - Thought to be the result of dust accumulating in dead zones of filter
- Important design parameter appears to be U/U_{mf} in the downcomer of the filter
 - Should be less than unity

Similitude analysis demonstrated here should be useful for purposes of estimating filter design at high temperatures and pressures as well as suggested operating conditions of prototypes even though scaling laws for collection efficiency were only tested here for modest pressures at room temperature, Table 2. Fly ash cleaning efficiencies of 99% and greater combined with the modest pressure drops (< 6.9 kPa (1.0 psi)) across the bed are encouraging for application in advanced coal-fired power cycles. The prospect that this granular filter can be used for simultaneous cleanup of solids and gases (SO_2 , H_2S) at high temperatures and pressures is being considered for future studies in which a suitable sorbent material is used in place of glass beads. A proposed calcium-based sorbet would have the following desirable characteristics: strong affinity for SO_2 , H_2S , regenerable and reusable, capable of dust removal, physically strong and attrition resistant, and low cost and long-lived.

Future Activities

The similitude predictions presented here require validation for scaling to high pressures and temperatures. Additional work is also needed to help understand particle transport and collection as follows: (1) confirmation of centerline particle sampling (present study) compared to full probe traverses for measuring total particle flow rates entering and leaving the bed; (2) profile sampling of collected dust within the granular bed itself to understand particle capture. In the present study, a borescope (fiber optic) was used for visual observations at the bed surface interface and for interior

inspection of the bed to a distance of a few centimeters. A detailed examination of the dust collection profile within the bed would help answer questions associated with conditions for caking, interior bed collection, particle coating etc. and non-optimum long-time increases in pressure drop across the bed. A future proposed study of simultaneous cleanup of solids and gases, SO₂, H₂S, with granular sorbent material will involve a high temperature facility operating at 800-1000 °C. Future industrial collaborative developments are also being explored using this technology for hot vapor clean-up of pyrolysis oils and possible licensing of technology.

References

Freidlander, S. K., 1977, *Smoke, Dust, and Haze*, John Wiley & Sons, NY.

Glicksman, L.R., M. Hyre, and K. Woloshun, 1993, *Powder Technology* 77: 177-199.

Mustonen, J. P., S. J. Bossart, and M. W. Durner, 1991, Technical and economical analysis of advanced particle filters for PFBC applications. *Proc. Int. Conf. on Fluidized Bed Combustion*, Montreal, Canada. Vol. 1: 475-480.

Saxena, S. C. et al., 1985, *Prog. Energy Combust. Sci.* 11: 193-251.

Shi, H., 2002, *Similitude Modeling and Experiments on a Moving Bed Granular Filter*, MS Thesis, Department of Mechanical Engineering, Iowa State University.

Soo, D., 2002, *Empirical Model Optimization of A Moving Bed Granular Filter for Particulate Removal*, MS Thesis, Department of Mechanical Engineering, Iowa State University.

Squires, A.M. and R. Pfeffer, 1970, *J. Air Pollut. Control Assoc.* 20: 534-538.

Vardeman, S. B., 1994, *Statistics for engineering problem solving*. Boston: PWS Publishing Company.

Wilson, K. B. and Hass, J. C., 1994, *Proc. Eleventh International Pittsburgh Coal Conference*, Pittsburgh, PA. Vol. 1: 131-136.

Figures and Tables

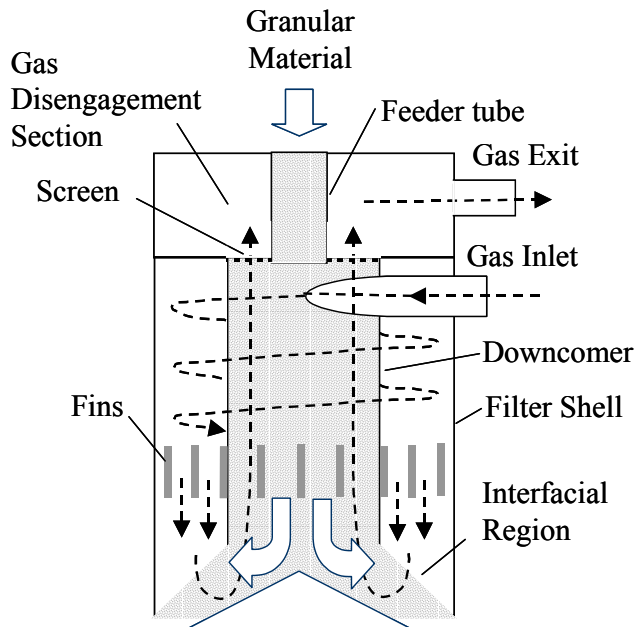


Fig. 1-a Counter-current flow moving Bbed granular filter



Fig. 1-b Photograph of granular bed.

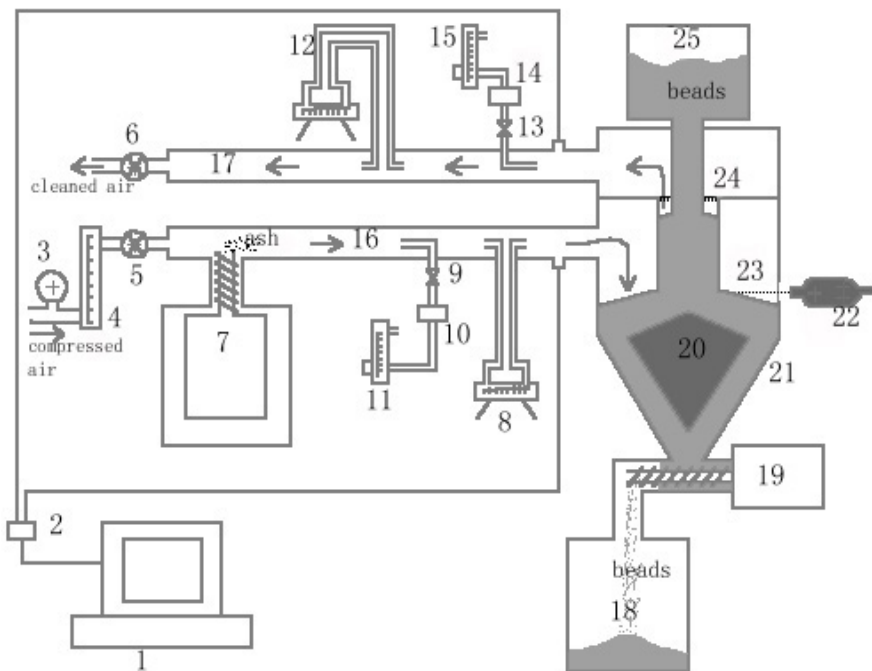


Fig. 2 Experimental setup - Counter-Current Flow Moving Bed Granular Filter

- 1 Computer
- 2 Pressure transducers
- 3 Pressure gage (0-100 psig)
- 4 Flowmeter (0-40 SCFM)
- 5 Inlet entrance control valve
- 6 Outlet exit valve
- 7 Ash feeder
- 8 Inlet S-type pitot tube
- 9 Inlet sampling probe
- 10 Inlet sampling filter
- 11 Inlet rotameter
- 12 Outlet S-type pitot tube
- 13 Outlet sampling probe
- 14 Outlet sampling filter
- 15 Outlet rotameter
- 16 Inlet pipe, 10.16 cm diameter
- 17 Outlet pipe, 10.16 cm diameter
- 18 Granule collection tank
- 19 Motor & auger system
- 20 Flow diverter
- 21 Moving bed filter body
- 22 Video camera
- 23 Granule downcomer
- 24 Metal screen
- 25 Granule hopper

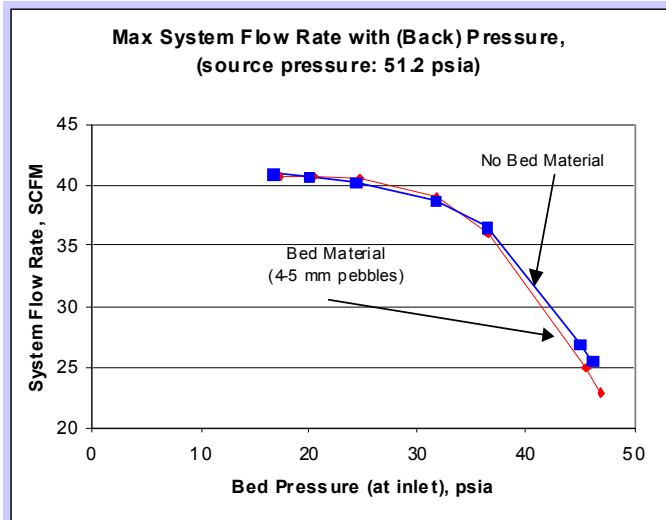


Fig. 3 Flow rate characteristics of filter system with/without pebbles against system pressure.



Fig. 4 (top) Wall deposition looking downstream at pitot tube; (bottom) deposition upstream at ash feeder



Fig. 5-a Dust cake at bed surface interface viewed through borescope.



Fig 5-b Clean particles below bed surface interface viewed through borescope (single 4 mm particle outline lower right).

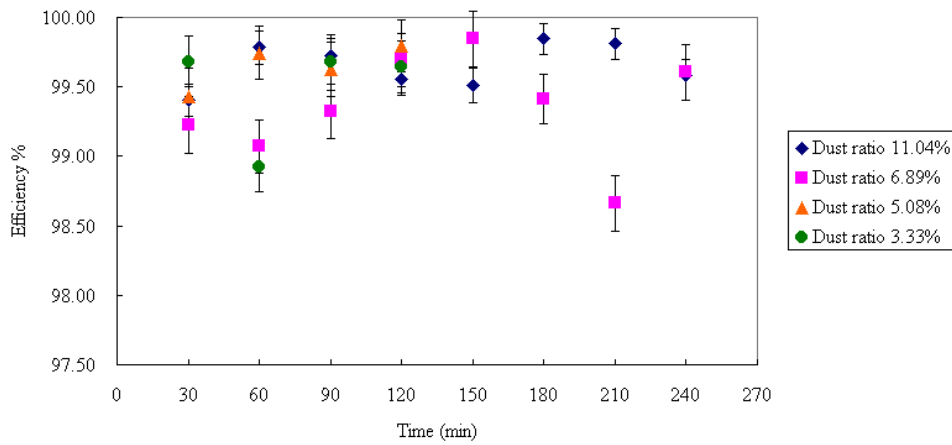


Fig. 6 Filter collection efficiency vs. time for four similitude experiments with different mass dust ratios (cf. Table 2) - bed: 4 mm spherical glass particles.

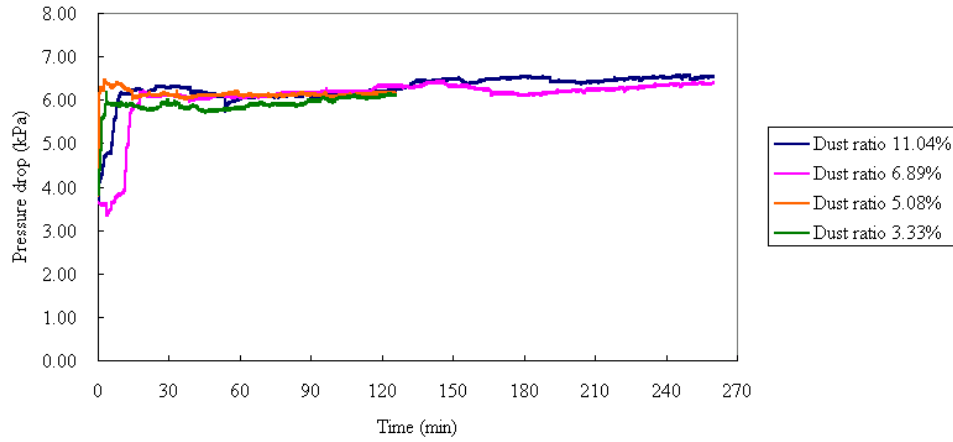


Fig. 7 Pressure drop vs. time for four similitude experiments with different mass dust ratios (cf. Table 2) - bed: 4 mm spherical glass particles.

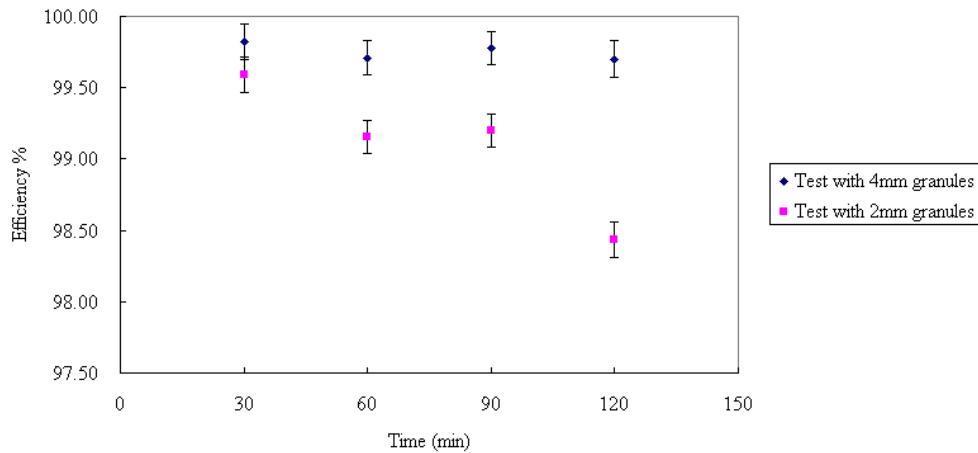


Fig. 8 Filter collection efficiency vs. time for experiment with 4 mm and 2 mm spherical glass beads.

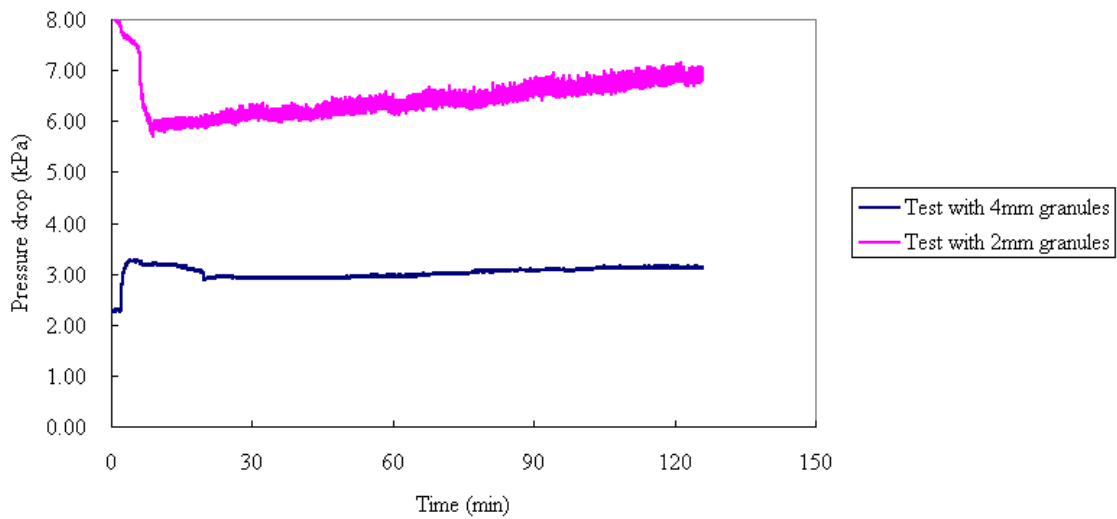


Fig. 9 Pressure drop vs. time for experiment with 4 mm and 2 mm spherical glass beads.

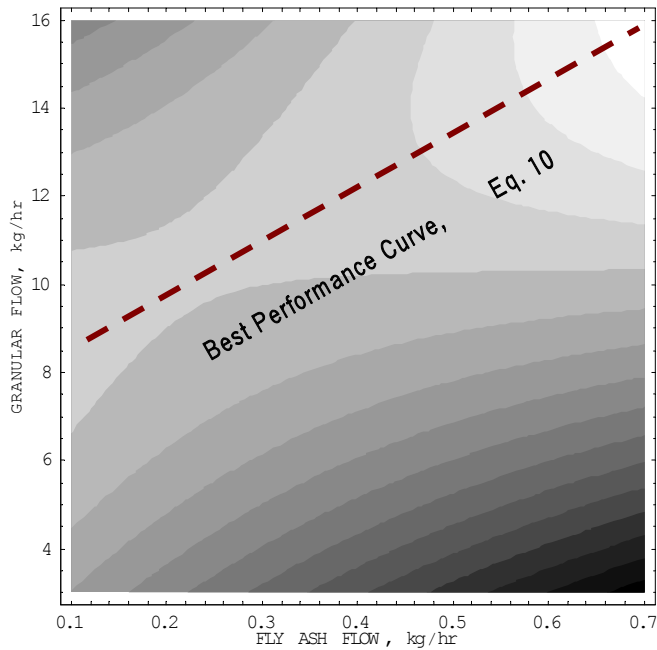


Fig. 10-a Particle collection efficiency (constant contour lines) as function of bed granular and fly ash flow rates; dark shading $\approx 96\%$, light shading $\approx 100\%$: superficial velocity 0.16 m/s.

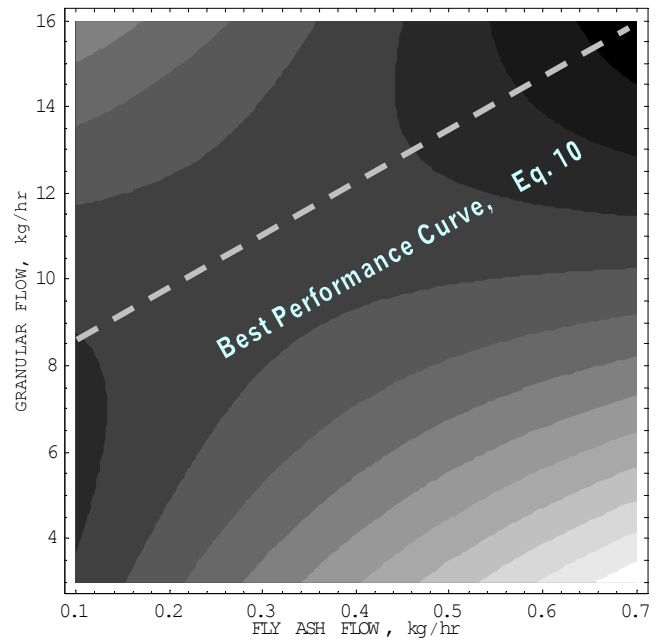


Fig. 10-b Pressure drop (constant contour lines) as function of bed granular and fly ash flow rates; dark shading ≈ 0.79 kPa (0.1 psid), light shading ≈ 3.4 kPa (0.5 psid).

Table 1. Achieving similitude (example) between granular filters, prototype and model

<i>Filter</i>	<i>Pressure</i> (kPa)	<i>Temp</i> (K)	<i>Gas Velocity</i> (cm/s)	<i>Dust</i> (microns)	<i>Granules</i> (microns)
Prototype	1031	1088	5	5	2000
Model	284	300	3.7	2.8	1100

<i>Filter</i>	<i>Re</i>	<i>St</i>	<i>R</i>	<i>Fr</i>	ρ_g/ρ_f
Prototype	7.3	0.0040	0.0025	0.13	790
Model	7.3	0.0041	0.0025	0.13	790

Table 2 Experimental conditions and dimensionless numbers for four similitude experiments (bed: 4 mm glass spheres)

Ash flow rate (g/min)	Granule flow rate (g/min)	Mass dust ratio %	Bed pressure kPa gage (psig)	Actual air density (kg/m ³)	Superficial U (m/s)	St	Re	R	R _{rho}	Fr
N/A	N/A	N/A	898.67 (130.34)	3.10	0.27	0.10	135.92	0.0029	790.32	1.02
11.12	100.77	11.04	157.65 (22.87)	3.08	0.20	0.10	135.01	0.0029	795.45	1.02
6.81	98.85	6.89	157.13 (22.79)	3.07	0.20	0.10	134.58	0.0029	798.05	1.02
10.48	206.35	5.08	159.66 (23.16)	3.10	0.20	0.10	135.89	0.0029	790.32	1.02
7.13	214.29	3.33	158.42 (22.98)	3.09	0.20	0.10	135.45	0.0029	792.88	1.02

Table 3 Average Particle Collection Efficiency obtained from each run

Run Number	Granular Flow Rate (GF), kg/hr	Superficial Velocity (VL), m/s	Dust Feed Rate (DL), kg/hr	¹ Average Efficiency (AE), %	Average Pressure Drop (APD), psid
1	6.85	0.175	0.2412	98.7	0.410188
2	13.10	0.176	0.1712	99.1	0.400224
3	6.80	0.213	0.2556	99.2	0.592271
4	13.00	0.216	0.2289	99.2	0.594244
5	6.70	0.177	0.2680	96.9	0.431666
6	12.10	0.177	0.3160	99.2	0.402229
7	7.27	0.190	0.5698	97.6	2.417593
8	15.40	0.211	0.4257	100.0	0.583525
9	9.36	0.196	0.4417	99.9	0.491264
10	10.16	0.197	0.5219	99.2	0.529075
11	3.32	0.179	0.3973	92.7	2.081311
12	14.00	0.199	0.3932	100	0.503971
13	9.12	0.161	0.3764	99.4	0.251282
14	8.24	0.207	0.5734	94.4	1.517345
15	8.64	0.195	0.0786	99.7	0.483909
16	9.68	0.200	0.7437	99.5	0.539434

¹ Averaged over duration of run.